

# NMR-Based Structure Determination of an Intertwined Coordination Cage Resembling a Double Trefoil Knot\*\*

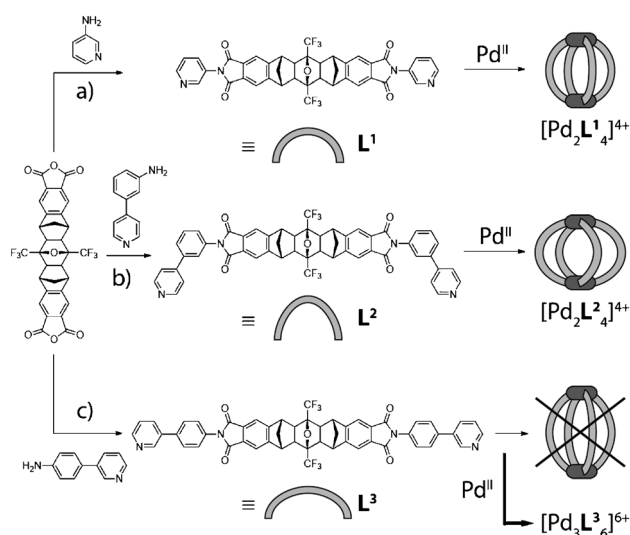
David M. Engelhard, Sabrina Freye, Kristof Grohe, Michael John, and Guido H. Clever\*

Understanding and controlling the topology of self-assembled structures plays a fundamental role in supramolecular chemistry. Especially the topologically nontrivial knot structures have attracted tremendous interest, not least because of their aesthetic appeal.<sup>[1]</sup> Important representatives that were synthesized during the last decades include the Hopf link (2-catenane),<sup>[2]</sup> the trefoil knot,<sup>[3]</sup> Solomon's link,<sup>[4]</sup> the pentafoil knot,<sup>[5]</sup> and Borromean rings.<sup>[6]</sup> In combination with well-defined cavities inside supramolecular cages,<sup>[7]</sup> the chiral and/or low-symmetric environment imposed by such nontrivial topologies may further contribute to the developments in the field of enzyme-like nanoreactors.<sup>[8]</sup>

Two general synthetic approaches towards coordination-chemistry-based knots can be distinguished by the role of the incorporated metal ions: The more established one uses the metal ions as templates,<sup>[1,6,9,10]</sup> whereas in the second approach, the coordinating metal ions are used as integral parts of the interwoven supramolecular assembly. Although numerous structurally simple coordination cages as well as metal-organic catenanes and rotaxanes are based on the second principle,<sup>[1b,11,12]</sup> the number of reported higher order knot and link structures following this pattern is still limited.<sup>[13]</sup> Structurally related, but topologically different, are interpenetrated coordination cages in which two or more metal-mediated cages form an interdigitated assembly without covalent or direct dative bonding between the cages.<sup>[14]</sup>

Sometimes, subtle changes in the design of a ligand that is known to form a topologically simple supramolecular assembly can result in the formation of a thermodynamic product of dramatically different structure. Herein we report on such an unexpected finding and its structural characterization by the interplay of high-resolution mass spectrometry, sophisticated NMR techniques, and computer-aided modeling.

As was previously shown, the self-assembly of rigid bis-monodentate pyridyl ligands **L**<sup>1</sup> with [Pd(CH<sub>3</sub>CN)<sub>4</sub>](BF<sub>4</sub>)<sub>2</sub> leads to a non-intertwined coordination cage of the composition [Pd<sub>2</sub>L<sub>4</sub>]<sup>4+</sup> (Scheme 1 a).<sup>[15,16]</sup> This architecture enables the encapsulation of differently sized dianionic guests and,



**Scheme 1.** Synthesis of short ligand **L**<sup>1</sup> (a) and the isomeric ligands **L**<sup>2</sup> (b) and **L**<sup>3</sup> (c) followed by their reaction with Pd<sup>II</sup> ions in acetonitrile to give the globular coordination cage [Pd<sub>2</sub>L<sub>4</sub>]<sup>4+</sup>, the widened derivative [Pd<sub>2</sub>L<sub>4</sub>]<sup>4+</sup>, and the unexpected compound [Pd<sub>3</sub>L<sub>6</sub>]<sup>6+</sup>, respectively (counterion in all cases: BF<sub>4</sub><sup>−</sup>).

depending on the guest size, the discrimination between discrete host-guest arrangements and chainlike oligomeric structures.<sup>[17]</sup> Based on this principle, novel pH-switchable (pseudo-)rotaxanes,<sup>[12]</sup> a system capable of light-triggered crystallization,<sup>[18]</sup> and discrete assemblies of Magnus' Salt-type stacked platinum compounds were developed.<sup>[19]</sup>

In order to incorporate larger molecules or to increase the guest/host ratio, control of the cavity size is a crucial prerequisite. We therefore prepared two new isomeric ligands expected to either widen (**L**<sup>2</sup>) or elongate (**L**<sup>3</sup>) the proposed cage compounds (Scheme 1 b,c), which was indeed the case with ligand **L**<sup>2</sup> (see the Supporting Information).

In contrast, ligand **L**<sup>3</sup> was surprisingly found to result in the clean formation of a structurally more complicated assembly composed of six ligands and three metal ions. The formula [Pd<sub>3</sub>L<sub>6</sub>]<sup>6+</sup> was unambiguously proven by the high-resolution mass spectrometry (HRMS) (see the Supporting Information).

The <sup>1</sup>H NMR spectroscopic study of the formation of complexes [Pd<sub>2</sub>L<sub>4</sub>]<sup>4+</sup> from **L**<sup>2</sup> and [Pd<sub>3</sub>L<sub>6</sub>]<sup>6+</sup> from **L**<sup>3</sup> shows further dramatic differences. Upon addition of Pd<sup>II</sup> to a solution of **L**<sup>2</sup> in CD<sub>3</sub>CN, the pyridine proton signals shift to lower field within 10 min, which is characteristic for the quantitative formation of the coordination cage (Figure 1 a). Similar to the reaction of **L**<sup>1</sup> with Pd<sup>II</sup> to give cage [Pd<sub>2</sub>L<sub>4</sub>]<sup>4+</sup>,<sup>[15]</sup> no signal splitting occurred, thus indicating the

[\*] D. M. Engelhard, S. Freye, K. Grohe, Dr. M. John, Prof. Dr. G. H. Clever  
Institut für Anorganische Chemie  
Georg-August Universität Göttingen  
Tammannstrasse 4, 37077 Göttingen (Germany)  
E-mail: gclever@gwdg.de  
Homepage: <http://www.clever-lab.de>

[\*\*] This work was funded by the DFG IRTG 1422. We thank Dr. H. Frauendorf for the HRMS measurements and Prof. Dr. C. Griesinger (MPI Göttingen) for access to his NMR facilities.

Supporting information for this article is available on the WWW under <http://dx.doi.org/10.1002/anie.201200611>.

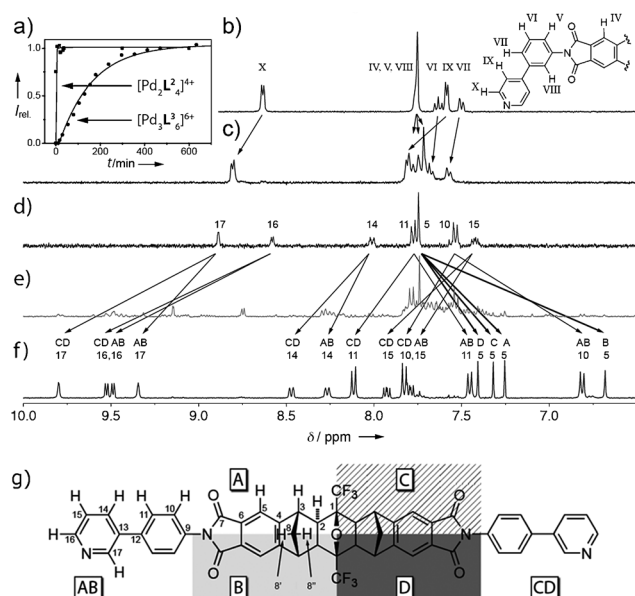


**Figure 1.** a) Time-dependent formation of  $[\text{Pd}_2\text{L}_2]^{4+}$  and  $[\text{Pd}_3\text{L}_3]^{6+}$ .  $^1\text{H}$  NMR spectra (400 MHz,  $\text{CD}_3\text{CN}$ ) at 333 K of b) ligand  $\text{L}^2$ , c) cage  $[\text{Pd}_2\text{L}_2]^{4+}$ , d) ligand  $\text{L}^3$ , e) intermediate mixture 17 min after metal addition, and f) the final product  $[\text{Pd}_3\text{L}_3]^{6+}$  after heating to  $60^\circ\text{C}$  for 12 h. g) Depiction of the low-symmetry environment around ligand  $\text{L}^3$  and signal assignment. Only a  $\text{C}_1$ -symmetric environment of  $\text{L}^3$  in  $[\text{Pd}_3\text{L}_3]^{6+}$ , in which all six ligands are equivalent (but completely asymmetrically surrounded by the remaining supramolecular structure), is consistent with all 1D and 2D  $^1\text{H}$ ,  $^{13}\text{C}$ , and  $^{19}\text{F}$  NMR data.

preservation of a high degree of symmetry (Figure 1b,c). In contrast, the reaction of  $\text{L}^3$  with  $\text{Pd}^{\text{II}}$  ions to give cage  $[\text{Pd}_3\text{L}_3]^{6+}$  requires more than 10 h to reach completion at  $60^\circ\text{C}$  (Figure 1a). This remarkably slow formation of the thermodynamic product already indicates that cage  $[\text{Pd}_3\text{L}_3]^{6+}$  has high structural complexity, since the rapid formation of cages of simpler structure, such as  $[\text{Pd}_2\text{L}_2]^{4+}$  from a similar bispyridyl ligand and the  $[\text{Pd}(\text{CH}_3\text{CN})_4](\text{BF}_4)_2$  precursor, reflects the fast ligand exchange that is to be expected in such a system. Moreover, in stark contrast to the observations made for  $[\text{Pd}_2\text{L}_2]^{4+}$  and  $[\text{Pd}_2\text{L}_2]^{4+}$ , the  $^1\text{H}$  NMR signals of the ligand in cage  $[\text{Pd}_3\text{L}_3]^{6+}$  split into sets of four (ligand backbone) and two (*p*-(3-pyridyl)phenyl donor sites), all of equal integration values. This indicates a reduction of the ligand's local symmetry. Worth mentioning is, furthermore, the observation of significant up- or downfield shifts for a number of backbone signals, which is another indicator for close contacts between the ligands inside a highly entangled structure.

Among the four symmetry proposals for possible ligand environments leading to the signal splitting found for  $[\text{Pd}_3\text{L}_3]^{6+}$ , three can be ruled out because of the number of observed signals and coupling patterns in the  $^1\text{H}$ ,  $^{19}\text{F}$ , and HMBC NMR spectra (Supporting Information, Figure S1). The only remaining possibility, an environment of four distinguishable quadrants A, B, C, and D around  $\text{L}^3$ , is depicted in Figure 1g. The full assignment of all aromatic  $^1\text{H}$  NMR signals is given in Figure 1f (see the Supporting Information for  $^{19}\text{F}$ ,  $^{13}\text{C}$ , and various 2D NMR spectra).

In order to identify a plausible structure of  $[\text{Pd}_3\text{L}_3]^{6+}$  in solution, it is now necessary to deduce and evaluate all possible topologically different assemblies fitting the formula  $[\text{Pd}_3\text{L}_3]^{6+}$ . If the six ligands are all chemically equal and the “principle of maximum site occupancy” is obeyed, the connecting  $\text{Pd}^{\text{II}}$  ions must be equivalent and therefore located on the corners of an equilateral triangle. This gives rise to seven different models as depicted in Figure 2. The non-

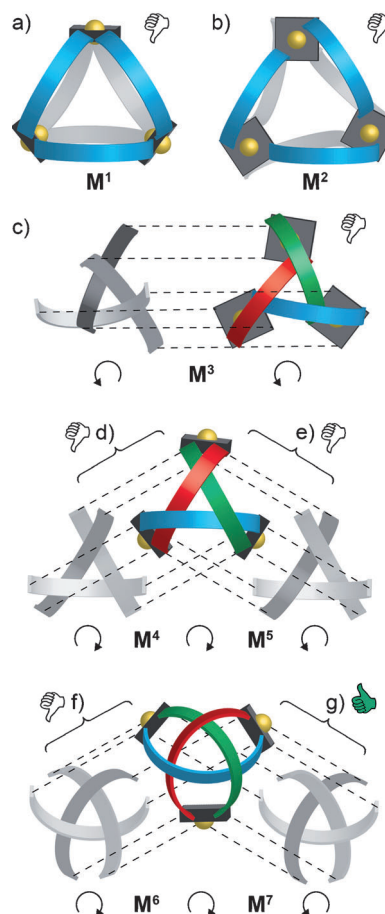


**Figure 2.** Among all possible topologies for a combination of six bis-monodentate ligands  $\text{L}^3$  and three square-planar-coordinated  $\text{Pd}^{\text{II}}$  ions in the assembly  $[\text{Pd}_3\text{L}_3]^{6+}$ , models  $\text{M}^1$ – $\text{M}^5$  (a–e) can be easily ruled out by symmetry considerations and NOE NMR analysis (see the Supporting Information). Chiral,  $D_3$ -symmetric model  $\text{M}^6$  and achiral,  $C_{3h}$ -symmetric model  $\text{M}^7$  (*meso*) are both assembled from two chiral trefoil-knot-shaped hemispheres to give a walnut-shaped structure. NOESY data, modeling results, and NMR titration experiments with a homochiral guest all support model  $\text{M}^7$  as the correct topology.

intertwined cases  $\text{M}^1$  (achiral, point group  $D_{3h}$ ) and  $\text{M}^2$  (chiral,  $D_3$ ) are inconsistent with the above-mentioned results (slow formation,  $^1\text{H}$  NMR signal shifting and splitting as a result of close interligand contacts). In the five intertwined structures  $\text{M}^3$ – $\text{M}^7$  ( $\text{M}^3$ ,  $\text{M}^4$ ,  $\text{M}^5$ : chiral  $D_3$ ;  $\text{M}^6$ ,  $\text{M}^7$  achiral  $C_{3h}$ ) the interligand H–H distances are expected to differ considerably. Indeed, comparison of the experimentally determined interligand distances obtained from the NOESY spectrum of  $[\text{Pd}_3\text{L}_3]^{6+}$  with the calculated distances obtained from un-

constrained semiempirical PM6 geometry optimizations<sup>[20]</sup> for all models gave crucial insight into the solution state structure (Figures S8 and S9).

Taken together, the NOE results were found to be consistent only with the chiral, walnut-shaped structure **M**<sup>6</sup> and, even better, with the related achiral structure **M**<sup>7</sup>: All observable interligand NOESY contacts were quantified by referencing them against a set of intraligand H–H distances of the rigid backbone of **L**<sup>1</sup> (obtained from the crystal structure of [Pd<sub>2</sub>**L**<sub>4</sub>]<sup>4+</sup>)<sup>[15]</sup> (see the Supporting Information). The comparison of the experimental with the calculated distances clearly shows that the double-trefoil-knot model **M**<sup>7</sup> correlates best, **M**<sup>6</sup> is slightly worse, and structures **M**<sup>1</sup>–**M**<sup>5</sup> show no correlation at all (Figures S11 and S12). As a further factor in favor of model **M**<sup>7</sup>, single-point energy calculations of the PM6 geometry-optimized models **M**<sup>6</sup> and **M**<sup>7</sup> at the DFT-B3LYP/LANL2DZ level indicate that model **M**<sup>7</sup> is 113.7 kJ mol<sup>−1</sup> lower in energy and thus the more stable structure. This energy difference may have its origin in the coordination geometries of the Pd<sup>II</sup> ions as calculated by the unconstrained structure optimizations: Whereas all {Pd-(pyridine)<sub>4</sub>} units of model **M**<sup>7</sup> converged to a perfectly square-planar geometry, they showed significant deviation from the perfect geometry in model **M**<sup>6</sup>.

Model **M**<sup>7</sup> is composed of two enantiomeric hemispheres, each in the shape of a trefoil knot, and it is thus achiral (*meso*). In order to obtain further evidence for the overall achiral nature of the proposed model, we titrated the cage compound with a solution of an enantiopure camphorsulfonate guest and monitored the reaction by <sup>1</sup>H NMR spectroscopy; the guest underwent quantitative encapsulation inside the cavity of structure **M**<sup>7</sup>.<sup>[21]</sup> HRMS data indicated the formation of a 1:1 host–guest adduct (see the Supporting Information). Both guest enantiomers show the same behavior: apart from the anticipated signal shift of certain protons belonging to the cage, no signal splitting could be observed upon addition of the chiral guest. This observation is also consistent with *meso* model **M**<sup>7</sup>, as the achiral structure should not discriminate between the two optical isomers of the chiral sulfonate. In contrast, a racemic mixture corresponding to the chiral model **M**<sup>6</sup> should show two different sets of signals for the diastereomeric matched and mismatched host–guest systems.

Figure 3 shows different representations of the PM6 geometry-optimized model **M**<sup>7</sup>, which is in full accordance with the [Pd<sub>3</sub>**L**<sub>6</sub>]<sup>6+</sup> composition (as elucidated by ESI-MS), all observed <sup>1</sup>H, <sup>19</sup>F, and <sup>13</sup>C NMR signal shifts, splittings, and couplings, as well as the values of the measured NOE contacts within experimental error, the relative DFT energies, and the test for chirality using a homochiral guest compound. Furthermore, the calculated model **M**<sup>7</sup> does not contain any chemically counterintuitive structural features, such as over-long bonds, overstretched angles, or improbably short non-covalent contacts (in contrast to the calculated structures of **M**<sup>3</sup>–**M**<sup>5</sup>, see the Supporting Information).

Comparison of the hydrodynamic radii obtained from DOSY (diffusion ordered spectroscopy) NMR spectra of all three coordination compounds measured in CD<sub>3</sub>CN shows, as expected, an increase in size in the order [Pd<sub>2</sub>**L**<sub>4</sub>]<sup>4+</sup> <

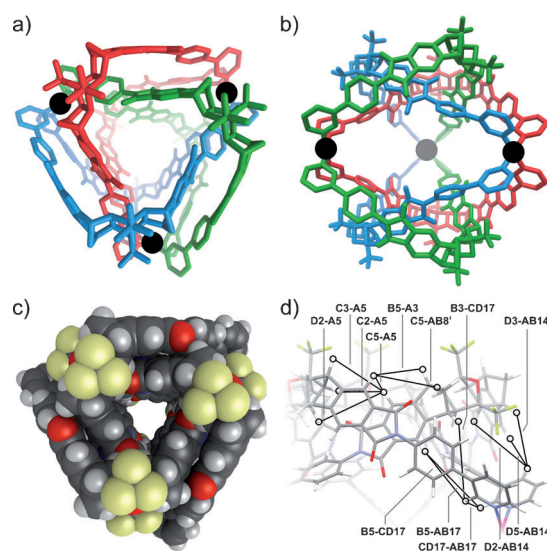


**Figure 3.** Stick models in a) top and b) side view (Pd ions highlighted as black spheres), and c) space-filling model of [Pd<sub>3</sub>**L**<sub>6</sub>]<sup>6+</sup> with a topology according to **M**<sup>7</sup> (PM6, Gaussian '09) based on 52 nonsymmetry-equivalent (40 nontrivial) NOESY contacts (overall 312). A selection of interligand contacts is depicted in (d). For further analysis, see the Supporting Information.

[Pd<sub>2</sub>**L**<sub>4</sub>]<sup>4+</sup> < [Pd<sub>3</sub>**L**<sub>6</sub>]<sup>6+</sup> (see the Supporting Information). The increase in size between [Pd<sub>2</sub>**L**<sub>4</sub>]<sup>4+</sup> and [Pd<sub>3</sub>**L**<sub>6</sub>]<sup>6+</sup>, however, is smaller than between [Pd<sub>2</sub>**L**<sub>4</sub>]<sup>4+</sup> and [Pd<sub>2</sub>**L**<sub>4</sub>]<sup>4+</sup> (although the increase in molecular mass is three times larger for the former than for the latter case) which can be well explained by the intertwined structure of model **M**<sup>7</sup> and the resulting dense packing within the supramolecular assembly.

This dense packing seems to be stabilized by six  $\pi$ – $\pi$  interactions between the phthalimide moieties in the backbones of adjacent ligands. Additional stabilization may arise from six hydrogen bonds between the B7 carbonyl oxygen atoms and the protons AB8-H' (distance: 2.3 Å). Indeed, in the <sup>1</sup>H NMR spectrum of [Pd<sub>3</sub>**L**<sub>6</sub>]<sup>6+</sup> this proton is shifted downfield by  $\delta$  = 0.4 ppm compared to the signal of the free ligand **L**<sup>3</sup>, whereas the signal of the outside-pointing proton AB8-H'' undergoes an upfield shift of  $\delta$  = 0.1 ppm (Supporting Information). Such an intertwined structure is not possible with ligand **L**<sup>2</sup> as the more angled structure disfavors close ligand proximity. Moreover, model **M**<sup>7</sup> indicates that **L**<sup>1</sup> is too short for such an entanglement.

In conclusion we were able to obtain, both a non-intertwined cage [Pd<sub>2</sub>**L**<sub>4</sub>]<sup>4+</sup> and an intertwined cage [Pd<sub>3</sub>**L**<sub>6</sub>]<sup>6+</sup> based on the subtle differences between the two isomeric ligands **L**<sup>2</sup> and **L**<sup>3</sup>. With the aid of HRMS and NMR techniques, one plausible solution-state structure for [Pd<sub>3</sub>**L**<sub>6</sub>]<sup>6+</sup> could be identified among several different coordination topologies. Correlation between measured NOE distances and those calculated from geometry-optimized models of all possible topologies suggests an achiral cage consistent with model **M**<sup>7</sup>. This unprecedented knot structure was further supported by the formation of a 1:1 host–guest complex with chiral camphorsulfonates.

We think that this double-trefoil-knot complex is a remarkable example of supramolecular architecture which adds to the few reported examples of knots in which the metal ions are not templates but integral parts of the structure.<sup>[1,13]</sup> Owing to the unique ribbonlike shape of the ligand backbone (with diagnostic protons located in all four distinct quadrants of the rigid structure but no rotational degrees of freedom) we were able to come up with a plausible solution structure based on NMR spectroscopic and mass spectrometric methods alone. Just as these methods have become indispensable for the structure elucidation of noncrystalline protein and nucleic acid structures in recent years,<sup>[22]</sup> the structural characterization of large supramolecular assemblies will surely profit from the further development of these techniques as well. Our present efforts are devoted to the idea of transferring other modern NMR techniques such as RDC (residual dipolar coupling)<sup>[23]</sup> to the field of supramolecular assembly.<sup>[24]</sup>

Furthermore, possible applications of the complex  $[\text{Pd}_3\text{L}_3]^{6+}$  can be seen in the fields of selective recognition and catalysis in confined environments. Currently, we are further exploring the host–guest chemistry and the control over the chirality of this walnut-shaped complex.

Received: January 21, 2012  
Published online: April 4, 2012

**Keywords:** host–guest systems · self-assembly · structure elucidation · supramolecular chemistry · trefoil knots

- [1] a) R. S. Forgan, J.-P. Sauvage, J. F. Stoddart, *Chem. Rev.* **2011**, *111*, 5434; b) J. E. Beves, B. A. Blight, C. J. Campbell, D. A. Leigh, R. T. McBurney, *Angew. Chem.* **2011**, *123*, 9428; *Angew. Chem. Int. Ed.* **2011**, *50*, 9260; c) C. A. Schalley, *Angew. Chem.* **2004**, *116*, 4499; *Angew. Chem. Int. Ed.* **2004**, *43*, 4399.
- [2] C. Dietrich-Buchecker, J. Sauvage, J. Kintzinger, *Tetrahedron Lett.* **1983**, *24*, 5095.
- [3] a) C. O. Dietrich-Buchecker, J.-P. Sauvage, *Angew. Chem.* **1989**, *101*, 192; *Angew. Chem. Int. Ed. Engl.* **1989**, *28*, 189; b) C. O. Dietrich-Buchecker, J. Guilhem, C. Pascard, J.-P. Sauvage, *Angew. Chem.* **1990**, *102*, 1202; *Angew. Chem. Int. Ed. Engl.* **1990**, *29*, 1154.
- [4] J. F. Nierengarten, C. O. Dietrich-Buchecker, J. P. Sauvage, *J. Am. Chem. Soc.* **1994**, *116*, 375.
- [5] a) J.-F. Ayme, J. E. Beves, D. A. Leigh, R. T. McBurney, K. Rissanen, D. Schultz, *Nat. Chem.* **2011**, *4*, 15; b) for the seminal work on this system see: B. Hasenknopf, J.-M. Lehn, N. Boumediene, A. Dupont-Gervais, A. van Dorsselaer, B. Kneisel, D. Fenske, *J. Am. Chem. Soc.* **1997**, *119*, 10956.
- [6] K. S. Chichak, *Science* **2004**, *304*, 1308.
- [7] a) D. M. Vriezema, M. Comellas Aragonès, J. A. A. W. Elemans, J. J. L. M. Cornelissen, A. E. Rowan, R. J. M. Nolte, *Chem. Rev.* **2005**, *105*, 1445; b) J. S. Dalgarno, N. P. Power, J. L. Atwood, *Coord. Chem. Rev.* **2008**, *252*, 825.
- [8] M. Yoshizawa, J. K. Klosterman, M. Fujita, *Angew. Chem.* **2009**, *121*, 3470; *Angew. Chem. Int. Ed.* **2009**, *48*, 3418.
- [9] M. Cesario, C. O. Dietrich-Buchecker, J. Guilhem, C. Pascard, J. P. Sauvage, *J. Chem. Soc. Chem. Commun.* **1985**, 244.
- [10] P. E. Barran, H. L. Cole, S. M. Goldup, D. A. Leigh, P. R. McGonigal, M. D. Symes, J. Wu, M. Zengerle, *Angew. Chem.* **2011**, *123*, 12488; *Angew. Chem. Int. Ed.* **2011**, *50*, 12280.
- [11] Representative examples: a) C. R. Woods, M. Benaglia, S. Toyota, K. Hardcastle, J. S. Siegel, *Angew. Chem.* **2001**, *113*, 771; *Angew. Chem. Int. Ed.* **2001**, *40*, 749; b) C. P. McArdle, J. J. Vital, R. J. Puddephatt, *Angew. Chem.* **2000**, *112*, 3977; *Angew. Chem. Int. Ed.* **2000**, *39*, 3819; c) F. Ibukuro, M. Fujita, K. Yamaguchi, J.-P. Sauvage, *J. Am. Chem. Soc.* **1999**, *121*, 11014.
- [12] G. H. Clever, M. Shionoya, *Chem. Eur. J.* **2010**, *16*, 11792.
- [13] a) T. K. Ronson, J. Fisher, L. P. Harding, P. J. Rizkallah, J. E. Warren, M. J. Hardie, *Nat. Chem.* **2009**, *1*, 212; b) F. Li, J. K. Clegg, L. F. Lindoy, R. B. Macquart, G. V. Meehan, *Nat. Commun.* **2011**, *2*, 205; c) O. V. Dolomanov, A. J. Blake, N. R. Champness, M. Schröder, C. Wilson, *Chem. Commun.* **2003**, 682; d) M. Schmittel, B. He, J. Fan, J. W. Bats, M. Engesser, M. Schlosser, H.-J. Deiseroth, *Inorg. Chem.* **2009**, *48*, 18192; e) J. Bourlier, A. Jouaiti, N. Kyritsakas-Gruber, L. Allouche, J.-M. Planeix, M. W. Hosseini, *Chem. Commun.* **2008**, 6191.
- [14] a) M. Fujita, N. Fujita, K. Ogura, K. Yamaguchi, *Nature* **1999**, *400*, 52; b) Y. Yamauchi, M. Yoshizawa, M. Fujita, *J. Am. Chem. Soc.* **2008**, *130*, 5832; c) J. J. Henkelis, T. K. Ronson, L. P. Harding, M. J. Hardie, *Chem. Commun.* **2011**, *47*, 6560; d) J. Heine, J. Schmedt auf der Günne, S. Dehnen, *J. Am. Chem. Soc.* **2011**, *133*, 10018; e) T. Hasell, X. Wu, J. T. A. Jones, J. Bacsá, A. Steiner, T. Mitra, A. Trewin, D. J. Adams, A. I. Cooper, *Nat. Chem.* **2010**, *2*, 750; f) A. Westcott, J. Fisher, L. P. Harding, P. Rizkallah, M. J. Hardie, *J. Am. Chem. Soc.* **2008**, *130*, 2950; g) M. Fukuda, R. Sekiya, R. Kuroda, *Angew. Chem.* **2008**, *120*, 718; *Angew. Chem. Int. Ed.* **2008**, *47*, 706; h) S. Freye, J. Hey, A. Torras-Galán, D. Stalke, R. Herbst-Irmer, M. John, G. H. Clever, *Angew. Chem.* **2012**, *124*, 2233; *Angew. Chem. Int. Ed.* **2012**, *51*, 2191.
- [15] G. H. Clever, S. Tashiro, M. Shionoya, *Angew. Chem.* **2009**, *121*, 7144; *Angew. Chem. Int. Ed.* **2009**, *48*, 7010.
- [16] For other examples of  $[\text{M}_2\text{L}_4]$ : a) N. Kishi, Z. Li, K. Yoza, M. Akita, M. Yoshizawa, *J. Am. Chem. Soc.* **2011**, *133*, 11438; b) P. Liao, B. W. Langloss, A. M. Johnson, E. R. Knudsen, F. S. Tham, R. R. Julian, R. J. Hooley, *Chem. Commun.* **2010**, *46*, 4932; c) N. L. S. Yue, D. J. Eisler, M. C. Jennings, R. J. Puddephatt, *Inorg. Chem.* **2004**, *43*, 7671; d) C.-Y. Su, Y.-P. Cai, C.-L. Chen, M. D. Smith, W. Kaim, H.-C. Zur Loye, *J. Am. Chem. Soc.* **2003**, *125*, 8595; e) D. K. Chand, K. Biradha, M. Fujita, *Chem. Commun.* **2001**, 1652; f) D. A. McMorran, P. J. Steel, *Angew. Chem.* **1998**, *110*, 3495; *Angew. Chem. Int. Ed.* **1998**, *37*, 3295.
- [17] G. H. Clever, W. Kawamura, M. Shionoya, *Inorg. Chem.* **2011**, *50*, 4689.
- [18] G. H. Clever, S. Tashiro, M. Shionoya, *J. Am. Chem. Soc.* **2010**, *132*, 9973.
- [19] G. H. Clever, W. Kawamura, S. Tashiro, M. Shiro, M. Shionoya, *Angew. Chem.* **2012**, *124*, 2660; *Angew. Chem. Int. Ed.* **2012**, *51*, 2606.
- [20] Gaussian09 (Revision A.1), M. Frisch, et al., Gaussian, Inc., Wallingford CT, **2009**. For the full citation see the Supporting Information.
- [21] For a 2:1 encapsulation of camphorsulfonate see: R. Sekiya, R. Kuroda, *Chem. Commun.* **2011**, *47*, 12346.
- [22] a) L.-Y. Lian, G. C. K. Roberts, *Protein NMR spectroscopy. Practical techniques and applications*, Wiley, Chichester, **2011**; b) C. Griesinger in *Essays in Contemporary Chemistry* (Eds.: G. Quinkert, M. V. Kisakürek), Verlag Helvetica Chimica Acta, Zürich, **2001**.
- [23] J. H. Prestegard, C. M. Bougault, A. I. Kishore, *Chem. Rev.* **2004**, *104*, 3519.
- [24] For a related example see: S. Sato, O. Morohara, D. Fujita, Y. Yamaguchi, K. Kato, M. Fujita, *J. Am. Chem. Soc.* **2010**, *132*, 3670.